

Developing Cross Section Sets for Fluorocarbon Etchants

Carl Winstead* and Vincent McKoy*

*A. A. Noyes Laboratory of Chemical Physics, California Institute of Technology, Pasadena, California 91125

Abstract. Successful modeling of plasmas used in materials processing depends on knowledge of a variety of collision cross sections and reaction rates, both within the plasma and at the surface. Electron–molecule collision cross sections are especially important, affecting both electron transport and the generation of reactive fragments by dissociation and ionization. Because the supply of cross section data is small and measurements are difficult, computational approaches may make a valuable contribution, provided they can cope with the significant challenges posed. In particular, a computational method must deal with the full complexity of low-energy electron–molecule interactions, must treat polyatomic molecules, and must be capable of computing cross sections for electronic excitation. These requirements imply that the method will be numerically intensive and thus must exploit high-performance computers to be practical. We have developed an *ab initio* computational method, the Schwinger multichannel (SMC) method, that possesses the characteristics just described, and we have applied it to compute cross sections for a variety of molecules, with particular emphasis on fluorocarbon and hydrofluorocarbon etchants used in the semiconductor industry. A key aspect of this work has been an awareness that cross section sets, validated when possible against swarm data, are more useful than individual cross sections. To develop such sets, cross section calculations must be integrated within a focused collaborative effort. Here we describe electron cross section calculations carried out within the context of such a focused effort, with emphasis on fluorinated hydrocarbons including CHF₃ (trifluoromethane), *c*-C₄F₈ (octafluorocyclobutane), and C₂F₄ (tetrafluoroethene).

INTRODUCTION

The critical importance of basic data to the understanding of plasma processes is well recognized (*e.g.*, [1]). In particular, it is apparent that numerical models of plasmas, regardless of their sophistication, cannot produce reliable output unless provided with reliable input. In materials-processing applications, many types of cross sections and reaction rates may be needed to understand the chemistry and physics within the plasma and at the surface, yet electron collision data have a special importance. Elastic electron cross sections are needed to model electron transport within the plasma, while inelastic cross sections, including those for electron-impact ionization and electronic excitation, are needed to understand the generation of reactive charged and neutral species. Yet the number of research groups engaged in the study of low-energy electron collisions in molecular gases is limited, and experimental measurement of neutral excitation and dissociation cross sections has proved very difficult. Computational approaches thus may play an important role.

CP636, *Atomic and Molecular Data and Their Applications: 3rd Int'l. Conf.*, edited by D. R. Schultz et al.
© 2002 American Institute of Physics 0-7354-0091-1/02/\$19.00

Computational study of low-energy electron–molecule collisions is in itself a significant challenge, especially where polyatomic molecules and inelastic processes are concerned. Methods developed for spherical targets (atoms) may prove inapplicable or slowly convergent when applied to molecular targets having low or no symmetry. Likewise, potential-scattering approaches, in which the problem is approximated as that of a single electron moving in an electric potential field, are economical and often successful for elastic scattering but are not readily applicable to electronic excitation (or ionization). Indeed, a general, flexible approach to low-energy electron–molecule collisions should be based on many-electron wavefunctions in order to account for the full quantum-mechanical complexity of the problem. Such a many-electron treatment can be numerically demanding, with the size of the calculation increasing rapidly as the number of electrons in the molecule increases. Therefore, numerical efficiency and an ability to exploit powerful computers are important considerations.

We have developed a computational method, the Schwinger Multichannel or SMC method [2, 3], that is specifically intended to treat inelastic as well as elastic collisions of low-energy electrons with polyatomic molecules, and we have adapted the SMC method to run efficiently on parallel computers [4, 5, 6, 7], which provide the resources necessary to carry out large-scale computations. We have applied the parallel SMC method to obtain elastic and inelastic electron cross sections for a variety of molecules, with generally good results [8, 9, 10, 11]. Yet we have come increasingly to appreciate that isolated cross section calculations, no matter their basic scientific interest, are of sharply limited utility to consumers of collision data, who usually desire cross section *sets* describing all of the principal electron-collision processes for a given molecule. Indeed, the ideal is a *self-consistent cross section set* (wherein, for example, the total collision cross section equals the sum of the partial cross sections) that has been *validated* against swarm data—that is, the swarm parameters (ionization coefficient, diffusion coefficients, etc.) calculated from the cross section set are in agreement with swarm or electron-drift measurements. Such a cross section set is a sounder basis for modeling than a collection of cross sections from various sources, which may (and often do) prove mutually inconsistent.

Here we review our participation in a research program directed primarily at obtaining electron collision data for fluoro- and hydrofluorocarbon etchants used in semiconductor fabrication. Our role has been to apply advanced computers and computational methods to obtain elastic and electron-impact excitation cross sections critical to the construction of validated cross section sets. In that role, we have collaborated with experimentalists having expertise in the measurement of ionization cross sections and swarm parameters, as well as with experts in the construction and validation of cross section sets and plasma chemistries.

The following section briefly describes our computational procedures. We then survey some recent results for fluoro- and hydrofluorocarbon gases and provide a few closing remarks.

COMPUTATIONAL METHOD

Detailed descriptions of both the SMC method [2, 3] and its implementation for parallel computers [6, 7] can be found elsewhere. Here we point out a few features that may be useful in appreciating the nature of the calculations and their scaling.

The SMC method is a first-principles variational method for the scattering amplitude, the quantity whose square modulus determines the cross section. By first principles, we mean that the SMC method is based directly on the electronic Schrödinger equation (or rather its integral-equation equivalent, the Lippmann–Schwinger equation); by variational, we mean that the SMC method finds, within a given space of possible wavefunctions describing the collision process, the wavefunction that gives the “best” scattering amplitude in a well-defined sense.

As is typical in computational applications of variational methods, we employ a linear expansion of the wavefunction—that is, we write it as a sum of known functions χ_i with unknown coefficients x_i . Introducing that form into the SMC variational expression for the scattering amplitude produces a system of linear equations,

$$\mathbf{A}\mathbf{x} = \mathbf{b}, \quad (1)$$

where \mathbf{A} is a known square matrix, \mathbf{b} is a known vector, and \mathbf{x} is the vector of unknowns x_i . Solving this equation by standard linear-algebraic techniques allows one to compute the variational approximation to the scattering amplitude.

In typical applications, the number of functions χ_i , and thus the dimension of the linear system of Eq. (1), ranges from about one hundred to a few thousand. Solving the linear system is thus not a major challenge. The real computational difficulty lies, rather, in the evaluation of the matrix \mathbf{A} and the vector \mathbf{b} . Let us focus on the elements of \mathbf{b} , because the most difficult part of \mathbf{A} involves elements of the same form; these elements are given by

$$b_i = \int d\tau \chi_i^* V \Phi(\vec{k}), \quad (2)$$

where the asterisk indicates complex conjugation, $d\tau$ indicates integration over all $3(N+1)$ coordinates of the N target electrons and the $(N+1)^{\text{th}}$ projectile electron, and V is the Coulombic interaction potential between the projectile electron and the electrons and nuclei of the target. $\Phi(\vec{k})$ is the product of an N -electron target wavefunction and a plane wave $\exp(i\vec{k} \cdot \vec{r}_{N+1})$ describing a free electron with momentum $\hbar\vec{k}$. Borrowing standard techniques of computational chemistry, we can approximate the target wavefunction contained in $\Phi(\vec{k})$ as a spin-adapted, antisymmetrized product of N one-electron functions ϕ_m (molecular orbitals) that are mutually orthogonal and are optimized to describe the electronic structure of the molecule. The functions χ_i are expanded similarly, using $(N+1)$ rather than N molecular orbitals. As a last step, the ϕ_m are written as linear combinations of functions chosen specifically to make ultimate evaluation of the integrals easier, namely, Cartesian Gaussians $g(\vec{r}; \alpha, \ell, m, n)$,

$$g(\vec{r}; \alpha, \ell, m, n) = C_{\alpha\ell mn} x^\ell y^m z^n \exp(-\alpha r^2), \quad (3)$$

$C_{\alpha\ell mn}$ being a normalization constant.

When these successive expansions are introduced into (2), \mathbf{b}_i reduces to a sum of integrals of two forms, the most numerous being

$$I_2 = \int d^3 r_1 \int d^3 r_2 g_\alpha(\vec{r}_1) g_\beta(\vec{r}_2) |\vec{r}_1 - \vec{r}_2|^{-1} g_\gamma(\vec{r}_1) \exp(i\vec{k} \cdot \vec{r}_2), \quad (4)$$

where we have for simplicity written $g_\alpha(\vec{r})$ for $g(\vec{r}; \alpha, \ell, m, n)$, etc. These integrals may be evaluated efficiently to high accuracy. The computational challenge arises, first, from their sheer number: if N_g is the number of Gaussians and N_k the number of plane waves, there are approximately $N_g^3 N_k / 2$ unique integrals of this type. For a larger molecule we might have $N_g \sim 500$ and $N_k \sim 100,000$, implying $\sim 10^{12}$ such integrals. The other computationally intensive step is combining these raw integrals with the coefficients of expansion that describe how the g_α form the ϕ_m and the ϕ_m form the χ_i to obtain matrix elements of \mathbf{b} and \mathbf{A} . One can show [6] that the number of arithmetic operations required is proportional to $N_g^4 N_k$. Because of the extra factor of N_g , transforming the raw integrals into final matrix elements will often, especially for larger molecules, require more computational effort than does evaluating them. Because total operation counts may lie in the range 10^{14} – 10^{15} , single-processor calculations would be tedious even with gigaflop (10^9 arithmetic operations per second) processors.

Fortunately, the two main computational steps are amenable to parallelization. It is obvious that evaluation of the raw integrals of (4) can be done in parallel—one only need assign each processor a different batch of integrals to evaluate. More care is required in the second step, where data must flow among processors in the course of the calculation. However, this step can be formulated [4] as multiplication of large, dense, distributed matrices, and parallel matrix multiplication is well-studied and inherently efficient. The SMC method is thus able to make efficient use of parallel computers and workstation clusters having dozens or hundreds of processors.

SELECTED RESULTS

In this section, we give an overview of results that we have recently obtained for CHF_3 (trifluoromethane), C_2F_4 (tetrafluoroethene), and $c\text{-C}_4\text{F}_8$ (octafluorocyclobutane). We have also studied a number of other fluoro- and hydrofluorocarbons, including C_2HF_5 (pentafluoroethane) [12], C_2F_6 (hexafluoroethane), C_6F_6 (hexafluorobenzene), 1,3- C_4F_6 (1,3-hexafluorobutadiene), and $c\text{-C}_5\text{F}_8$ (octafluorocyclopentene), as well as radicals such as CHF and CF_2 that may be present in plasmas at significant concentrations; however, the three examples we have chosen are fairly representative and are also of some current interest in plasma etching applications.

CHF_3

To aid in developing an electron cross section set for CHF_3 [13], we used the parallel SMC method described earlier to carry out calculations of the elastic cross section (differential, integral, and momentum transfer) as well as of the electron-impact exci-

tation cross sections for several low-lying electronic states. In addition to these collision calculations, we carried out ancillary studies of fragmentation energetics and of the dissociative behavior of some of the excited states using standard quantum chemistry methodology. We found that each of the excited states whose excitation cross section we considered was dissociative; though not unexpected, this was a useful result in that a major goal was to obtain an estimate of the total dissociation cross section.

Comparison to other calculated [14, 15] and experimental [15] results confirmed that our elastic cross sections were reasonably good. For the inelastic cross sections, whose sum is shown in Fig. 1, there are no data to which we may directly compare. However, measured values of the total neutral dissociation cross section that are far smaller than our calculated excitation cross section have been reported [16, 17]. Given the limited nature of the calculations, we would not expect the cross section of Fig. 1 to be a highly accurate approximation to the total neutral dissociation cross section, but we would expect it to provide a good starting point for estimating that cross section. Such a discrepancy between calculated and laboratory-based results exemplifies the need for further consistency checks in the construction of a cross section set.

Such a consistency check was provided by using the calculated cross sections, together with measured electron-impact ionization cross sections [18], to carry out a swarm analysis, in which electron transport coefficients obtained by simulations based on the cross sections are compared to the electron transport coefficients for CHF_3 obtained in swarm measurements [19, 20]. If significant discrepancies exist, the cross sections are adjusted systematically [21] to bring the simulation results into better agreement with the measured swarm data.

The swarm analysis, performed by our collaborator, W. L. Morgan, resulted in a total dissociation cross section that was larger by a factor of 1.4 than the summed excitation cross section of Fig. 1, thus confirming our suspicion that the measured dissociation cross sections are (for unknown reasons) far too small. Similar conclusions were reached in an independent swarm analysis performed at about the same time by Kushner and Zhang [22], though there were significant differences in other respects between the cross section set of Kushner and Zhang and ours.

c- C_4F_8

Octafluorocyclobutane, *c*- C_4F_8 , presents a significantly greater computational challenge than CHF_3 , as is readily seen if we recall that two the principal computational steps increase in difficulty in proportion to N_g^3 and N_g^4 , respectively, where N_g is the number of Cartesian Gaussian functions. Since N_g is in turn roughly proportional to the number of non-hydrogen atoms in the molecule, it is apparent that cross section calculations on *c*- C_4F_8 are inherently several dozen times more challenging than comparable calculations on CHF_3 . Nonetheless, by exploiting multiprocessor computers, calculations of useful quality could still be carried out with reasonable turnaround times. We obtained [23] differential, integral and momentum transfer elastic cross sections as well as cross sections for excitation of the lowest singlet and triplet excited electronic states.

In Fig. 2, the computed differential elastic cross section is shown at several energies in

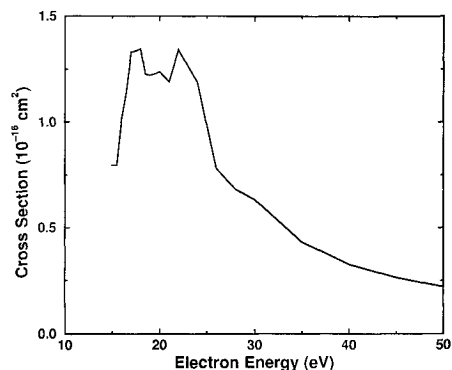


FIGURE 1. Summed cross sections for electronic excitation of CHF_3 , from Ref. [13].

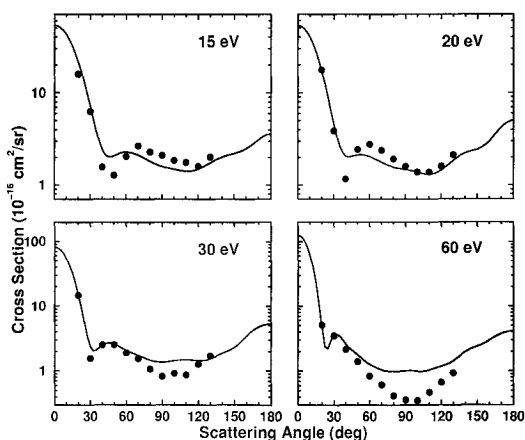


FIGURE 2. Differential elastic cross section for electron scattering by $c\text{-C}_4\text{F}_8$ at 15, 20, 30, and 60 eV. Experimental data (filled circles) are from Ref. [24]. Figure taken from Ref. [23].

comparison with experimental values obtained by Tanaka *et al.* [24]. The generally good agreement gives us confidence that our integral and momentum transfer cross sections (which are derived from the differential cross section) are reliable at these energies. At lower energies, agreement with the measured differential cross section is less good, for well-understood reasons. With additional computational effort, better low-energy results could be obtained; however, we were primarily interested in the energy range where excitation and ionization processes occur.

Font *et al.* [25] employed our calculated cross sections, along with ionization cross sections measured by Jiao *et al.* [26], to perform a swarm analysis similar to that previously described for CHF_3 . They then used the resulting cross section set, together with a plasma chemistry that they also developed, in simulations of a plasma reactor,

obtaining generally good agreement with diagnostic measurements for a variety of properties, including, for example, the densities of various radical fragments.

C_2F_4

Tetrafluoroethene (or tetrafluoroethylene), C_2F_4 , has attracted considerable recent interest as an etching gas; as Samukawa *et al.* have demonstrated [27], adjusting the proportions of C_2F_4 and CF_3I in a mixture affords a degree of control over the relative densities of CF_2 and CF_3 radicals, allowing optimization of the etching process. From a chemical point of view, C_2F_4 also forms an interesting contrast to CHF_3 and $c-C_4F_8$. C_2F_4 has a double bond consisting of C–C σ and π orbitals, and there are low-lying and strongly excited electronic states arising from excitation out of the π bonding orbital into the conjugate π^* antibonding orbital. One also expects temporary trapping of the scattering electron in the π^* orbital to give rise to a prominent resonance (peak) in the low-energy elastic cross section.

The moderate size and high symmetry of C_2F_4 are advantages to computations. It was consequently possible to do an unusually thorough study [28]. For the elastic cross sections, we included polarization effects, which were completely omitted in the studies of CHF_3 and $c-C_4F_8$, in the description of resonant scattering, in order to obtain better resonance energies. For electron-impact excitation, we computed cross sections not only for the $\pi \rightarrow \pi^*$ triplet (T) and singlet (V) states but also for eight other states that had fairly low excitation thresholds; although we neither expected nor found any of these states to be individually as important as either $\pi \rightarrow \pi^*$ state, they did turn out collectively to be significant contributors to the total excitation cross section.

Our elastic calculation placed the π^* resonance at 3.6 eV; dissociative attachment [29, 30, 31] and derivative-mode transmission [32] measurements variously place the resonance at 2.8 to 3.6 eV. Given the limitations of the calculation (in particular, the neglect of vibrational motion), we consider the agreement reasonably good. We likewise found that higher-energy resonances in the elastic cross section correlated rather well with known dissociative attachment features. The only elastic cross section measurements available for C_2F_4 appear to be the 1976 relative differential cross sections of Coggiola *et al.* [33]. If those data are placed on an absolute scale by single-point normalization to our calculations, generally good agreement is again found [28].

The cross sections for the T and V ($\pi \rightarrow \pi^*$) states are shown in Fig. 3. The cross section for excitation of the T state is considerably smaller than the V-state cross section, but the low threshold for excitation gives the T excitation channel special importance in low-temperature plasmas, where the peak in the electron energy distribution may lie at few eV or less. The magnitude of the V-state cross section is explained by the strong optical transition moment of the singlet state, which promotes excitation to the V state even in distant collisions with relatively fast-moving electrons. In Fig. 4, cross sections for eight additional states are shown. Comparison to Fig. 3 verifies that, as stated earlier, none has the low threshold of the T-state cross section nor the large magnitude of the V-state cross section, but that collectively their contribution to the total cross section is significant in a certain energy range, roughly 10–30 eV.

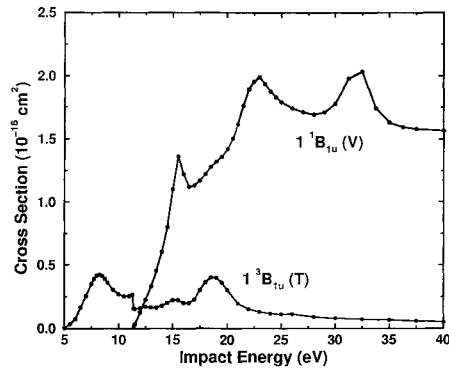


FIGURE 3. Integral cross sections for electron-impact excitation of the T (1^3B_{1u}) and V (1^1B_{1u}) states of C_2F_4 , from Ref. [28].

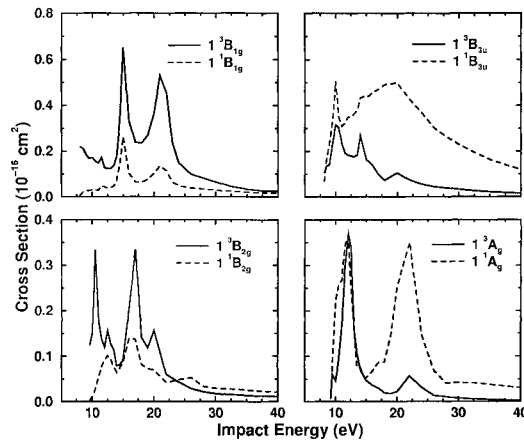


FIGURE 4. Integral cross sections for electron-impact excitation of eight low-lying electronic states of C_2F_4 , from Ref. [28].

A cross section set for C_2F_4 was constructed [34] based on the calculated cross sections just described and measured ionization cross sections obtained by Haaland and Jiao [35]. At the time we began work on C_2F_4 , no swarm data against which the cross section set might be validated were available, so the effort was extended to encompass swarm measurements by H. Tagashira, K. Yoshida, and S. Goto. W. L. Morgan once again carried out the swarm analysis necessary to produce a validated cross section set. One notable result of the swarm analysis was that it proved unnecessary to adjust the calculated cross sections in order to obtain good agreement with the measured swarm parameters. A second interesting observation was that the two-term Boltzmann analysis proved unreliable at higher values of E/N (the ratio of the applied field to the

number density); in other words, the momentum transfer cross section does not capture sufficient information about the anisotropy of the elastic scattering. A Monte-Carlo analysis employing the calculated differential elastic cross sections, however, proved quite successful [34].

CONCLUDING REMARKS

We hope that the examples presented above demonstrate the potential of first-principles calculations to make useful and timely contributions to the supply of critical electron-molecule collision data. We are keenly aware that such calculations are still limited in some important ways—for example, electronic excitation remains a difficult problem, as does elastic scattering at very low energies (~ 1 eV or less)—and we are working to address those limitations. Nonetheless, there is much that can be accomplished with current computational technology, and given the persistent dearth of experimental data for technologically important molecules, computation will continue to have an important role to play.

At the same time, we hope to have made clear that cross section calculations are most useful as a component in a coherent program directed at obtaining self-consistent cross section sets (and, where necessary, swarm data against which those sets may be validated). It is possible to compute cross sections only for some of the (infinite) excitation processes in a given molecule, though fortunately it is often possible to identify *a priori* those that will be most important, and the accuracy currently attainable remains limited. Thus, while computations can provide a starting point for developing an excitation/dissociation cross section, in the form of the energy dependence and approximate magnitude of the cross section, validation against swarm measurements, and adjustment where necessary, remain essential steps. Likewise, some processes, such as electron-impact ionization of polyatomic molecules, remain out of reach of present first-principles computational techniques; despite the many successes of simple approximations such as the BEB model [36] and the modified additivity rule [37], measurements of these cross sections are the preferable alternative, especially as they can provide cross sections for individual fragment ions. As logic would suggest, critical data needs can be addressed most efficiently through a pragmatic approach that draws upon the best features of computation, experiment, and simulation.

ACKNOWLEDGMENTS

It is a pleasure to acknowledge collaboration with W. L. Morgan, P. D. Haaland, and their co-workers throughout the work described herein, as well as with H. Tagashira, K. Yoshida, and S. Goto in the development of a C_2F_4 cross section set. Work at Caltech was supported by Sematech, Inc., by the Department of Energy through the Office of Basic Energy Sciences, and by an equipment grant from Intel Corp. Calculations made use of the facilities of the Caltech Center for Advanced Computing Research and of the Jet Propulsion Laboratory's Supercomputing Project.

REFERENCES

1. Tanaka, H., and Inokuti, M., *Adv. At., Mol., Opt. Phys.* **43**, 1–16 (2000).
2. Takatsuka, K., and McKoy, V., *Phys. Rev. A* **24**, 2473–2480 (1981).
3. Takatsuka, K., and McKoy, V., *Phys. Rev. A* **30**, 1734–1740 (1984).
4. Hipes, P., Winstead, C., Lima, M., and McKoy, V., “Studies of Electron-Molecule Collisions on the Mark IIIfp Hypercube,” in *Proceedings of the Fifth Distributed Memory Computing Conference, Charleston, SC, Vol. I: Applications*, edited by D. W. Walker and Q. F. Stout, IEEE Computer Society, Los Alamitos, California, 1990, pp. 498–503.
5. Winstead, C., Hipes, P. G., Lima, M. A. P., and McKoy, V., *J. Chem. Phys.* **94**, 5455–5461 (1991).
6. Winstead, C., and McKoy, V., *Adv. At., Mol., Opt. Phys.* **36**, 183–219 (1996).
7. Winstead, C., and McKoy, V., *Comput. Phys. Commun.* **128**, 386–398 (2000).
8. Winstead, C., and McKoy, V., *Adv. Chem. Phys.* **96**, 103–190 (1996).
9. Winstead, C., and McKoy, V., *Phys. Rev. A* **57**, 3589–3597 (1998).
10. Lee, C.-H., Winstead, C., and McKoy, V., *J. Chem. Phys.* **111**, 5056–5066 (1999).
11. Bettega, M. H. F., Winstead, C., and McKoy, V., *J. Chem. Phys.* **112**, 8806–8812 (2000).
12. Bettega, M. H. F., Winstead, C., and McKoy, V., *J. Chem. Phys.* **114**, 6672–6678 (2001).
13. Morgan, W. L., Winstead, C., and McKoy, V., *J. Appl. Phys.* **90**, 2009–2016 (2001).
14. Natalense, A. P. P., Bettega, M. H. F., Ferreira, L. G., and Lima, M. A. P., *Phys. Rev. A* **59**, 879–881 (1999).
15. Varela, M. T. do N., Winstead, C., McKoy, V., Kitajima, M., and Tanaka, H., *Phys. Rev. A* **65**, 022702 (2002).
16. Goto, M., Nakamura, K., Toyoda, H., and Sugai, H., *Jpn. J. Appl. Phys.* **33**, 3602–3607 (1994).
17. Sugai, H., Toyoda, H., Nakano, T., and Goto, M., *Contrib. Plasma Phys.* **35**, 415–420 (1995).
18. Jiao, C. Q., Nagpal, R., and Haaland, P. D., *Chem. Phys. Lett.* **269**, 117–121 (1997).
19. Wang, Y., Christophorou, L. G., Olthoff, J. K., and Verbrugge, J. K., *Chem. Phys. Lett.* **304**, 303–308 (1999).
20. de Urquijo, J., Alvarez, I., and Cisneros, C., *Phys. Rev. E* **60**, 4990–4992 (1999).
21. Morgan, W. L., *J. Phys. D* **26**, 209–214 (1993).
22. Kushner, M. J., and Zhang, D., *J. Appl. Phys.* **86**, 3231–3234 (2000).
23. Winstead, C., and McKoy, V., *J. Chem. Phys.* **114**, 7407–7412 (2001).
24. Tanaka, H., private communication.
25. Font, G. I., Morgan, W. L., and Mennenga, G., *J. Appl. Phys.* **91**, 3530–3538 (2002).
26. Jiao, C. Q., Garscadden, A., and Haaland, P. D., *Chem. Phys. Lett.* **297**, 121–126 (1998).
27. Samukawa, S., Mukai, T., and Tsuda, K., *J. Vac. Sci. Technol. A* **17**, 2551–2556 (1999).
28. Winstead, C., and McKoy, V., *J. Chem. Phys.* **116**, 1380–1387 (2002).
29. Thynne, J. C. J., and MacNeil, K. A. G., *Int. J. Mass Spectrom. Ion Phys.* **5**, 329 (1970).
30. Heni, M., Illenberger, E., Baumgärtel, H., and Süzer, S., *Chem. Phys. Lett.* **87**, 244–248 (1982).
31. Illenberger, E., Baumgärtel, H., and Süzer, S., *J. Electron Spectrosc. Relat. Phenom.* **33**, 123–139 (1984).
32. Chiu, N. S., Burrow, P. D., and Jordan, K. D., *Chem. Phys. Lett.* **68**, 121–126 (1979).
33. Coggiola, M. J., Flicker, W. M., Mosher, O. A., and Kuppermann, A., *J. Chem. Phys.* **65**, 2655 (1976).
34. Yoshida, K., Goto, S., Tagashira, H., Winstead, C., McKoy, B. V., and Morgan, W. L., *J. Appl. Phys.* **91**, 2637–2647 (2002).
35. Haaland, P. D., private communication.
36. Hwang, W., Kim, Y.-K., and Rudd, M. E., *J. Chem. Phys.* **104**, 2956–2966 (1996).
37. Deutsch, H., Becker, K., and Märk, T. D., *Int. J. Mass Spectrom.* **167**, 503–517 (1997).